

Wire electrical discharge machinability and load-bearing capacity of ATZ-WC composite ceramics

Marcel Olivier, Raphael Heß, Andrea Gommeringer, Frank Kern, Tim Herrig and Thomas Bergs

Marcel Olivier. Laboratory for Machine Tools and Production Engineering WZL of RWTH Aachen University, Campus-Boulevard 30, 52074 Aachen, Germany

Corresponding author: M.Olivier@wzl.rwth-aachen.de

Raphael Heß. Laboratory for Machine Tools and Production Engineering WZL of RWTH Aachen University, Campus-Boulevard 30, 52074 Aachen, Germany

Andrea Gommeringer. Institute for Manufacturing Technologies of Ceramic Components and Composites (IFKB), University of Stuttgart, Allmandring 7b, 70569 Stuttgart, Germany

Frank Kern. Institute for Manufacturing Technologies of Ceramic Components and Composites (IFKB), University of Stuttgart, Allmandring 7b, 70569 Stuttgart, Germany

Tim Herrig. Laboratory for Machine Tools and Production Engineering WZL of RWTH Aachen University, Campus-Boulevard 30, 52074 Aachen, Germany

Fraunhofer Institute for Production Technology IPT, Steinbachstraße 17, 52074 Aachen, Germany

Thomas Bergs. Laboratory for Machine Tools and Production Engineering WZL of RWTH Aachen University, Campus-Boulevard 30, 52074 Aachen, Germany

Fraunhofer Institute for Production Technology IPT, Steinbachstraße 17, 52074 Aachen, Germany

Abstract. Electrically conductive and thereby electrical discharge machinable ceramics may gain further relevance for tooling applications and in chemical industry. They combine high chemical and thermal durability with high hardness and strength. While these properties represent a significant advantage for application, they are a major challenge for conventional machining. Due to the thermophysical removal principle, wire electrical discharge machining (WEDM) is a suitable manufacturing process for hardness-independent machining and may broaden the use of ceramics especially in case of customized complex parts. Up to now, there are only a few investigations on WEDM of electrically conductive ceramics, especially with regard to the surface integrity and the influence of the EDM process on the mechanical properties. A previous study investigated the influence of different WEDM technologies on the surface integrity and the resulting load-bearing capacity of a zirconia-tungsten carbide (TZP-WC) ceramic. Based on this investigation, the heat flow in this ceramic composite was calculated with the use of a heat simulation model and compared with the analyzed rim zone, in order to predict a priori reliable process parameters. Furthermore, the wire electrical machinability and the bending strength of alumina-zirconia-tungsten carbide (ATZ-WC) composite ceramics with different fractions of the respective phases were investigated to identify the correlations and verify the simulation model.

Keywords. Electrical Discharge Machining, Ceramics, Load-Bearing Capacity, Modelling

1 Introduction

High performance structural ceramics are successfully implemented in application fields such as mechanical engineering and biomedical industry, where their favorable properties, mechanical strength and hardness, high temperature stability and chemical inertness are required. Their high hardness and abrasion resistance, however, make conventional final machining costly and time consuming, so that typical ceramic production cycles either follow a net shaping strategy or are based on a “green (i.e. non sintered) machining” of blanks. For customized components of high complexity these manufacturing strategies are often either not applicable for economic reasons or technically not feasible as some geometric features are impossible. Additive manufacturing technologies are rapidly developing, to date the AM manufactured parts do not yet fulfill extreme demands concerning strength and dimensional tolerances. Electrical discharge machining (EDM) of ceramics may fill this gap, provided that an electrically conductive ($\kappa > 1 -$

10 S/m, [1]) and thereby ED-machinable ceramic is available and the EDM process parameters are properly set up to be able to fully exploit the potential of the material. Although ED-machinability has been investigated for different ceramics in various studies, there is still a demand to investigate the effect of EDM on ceramics and their mechanical properties. The publications of Ferraris and Pachaury give an overview of EDM processing of various ceramics [2,3]. In most investigations, the main focus was the analysis of the material removal mechanism [4,5]. Studies on the effect of EDM on the mechanical properties of ceramics are rare [6]. Furthermore, typically either sink EDM in oil-based dielectric or wire EDM in water-based dielectric was used. Klocke et al. were able to show that machining ceramics with wire EDM in oil-based dielectric leads to less surface damage than sink EDM or wire EDM in water-based dielectric [7]. For this reason, Bergs et al. investigated the influence of wire EDM on the surface integrity and mechanical load capacity of zirconia-tungsten carbide (TZP-WC) ceramics using an oil-based dielectric [8]. In this study the influence of wire EDM on the load-bearing capacity of alumina-zirconia-tungsten carbide (ATZ-WC) composite ceramics with different fractions of alumina is investigated. Moreover, a thermal simulation model is developed and validated based on the previous results in order to estimate a priori reliable process parameters for the machining of further ceramic compositions with different discharge parameters.

2 Experimental setup

The investigated material system consists of an oxide matrix, co-stabilized tetragonal zirconia with alumina (0.5 – 10 vol.%), and an electrically conductive carbide dispersion (nanoscale tungsten carbide, 28 – 36 vol.%). The tetragonal phase of zirconia was stabilized by 1.5 mol% yttrium oxide and 1.5 mol% neodymium oxide (Y,Nd-TZP). The starting powders for the mixed ceramics, consisting of zirconium oxide (TZ-0, Tosoh), alumina (APA0.5, Ceralox), tungsten carbide (WC DN4.0, H.C. Starck), as well as the stabilizers yttrium oxide (Y₂O₃ nanopowder, Chempur) and neodymium oxide (Nd₂O₃ nanopowder, Chempur), were intensively ground together on a stirred ball mill (cover grinding). The exact powder preparation methods are described in detail elsewhere [9]. In the previous study [7], only one composition of the respective phases was investigated (0.5A-28WC). For this paper, the scope was broadened to twelve different compositions, which are listed in Table 1, in order to be able to precisely determine the influence of each phase.

Table 1: Matrix of the material system Y,Nd-TZP-WC

		Fraction of tungsten carbide		
		28 vol.% WC	32 vol.% WC	36 vol.% WC
Fraction of alumina	0.5 vol.% Al ₂ O ₃	0.5A-28WC	0.5A-32WC	0.5A-36WC
	2.5 vol.% Al ₂ O ₃	2.5A-28WC	2.5A-32WC	2.5A-36WC
	5.0 vol.% Al ₂ O ₃	5A-28WC	5A-32WC	5A-36WC
	10.0 vol.% Al ₂ O ₃	10A-28WC	10A-32WC	10A-36WC

The prepared powders were hot pressed (1400 °C, 2 h, 60 MPa) to form dense cylindrical discs ($\varnothing = 40$ mm, $h = 4$ mm). In preparation for electrical characterization, the specimens were deburred, lapped and polished (1 μ m). Bending strength tests were carried out in a four point setup with 20 mm outer and 10 mm inner span. For this purpose, $b_{\text{Bar}} = 2.3$ mm wide bending bars with a length of $l_{\text{Bar}} = 25$ mm were manufactured from each material by wire EDM. A Cut2000 X Oiltech (GF Machining Solutions), which uses an oil-based dielectric (IonoFil100, oelheld), was used as wire EDM machine. A brass wire with a diameter of $\varnothing_{\text{Wire}} = 0.2$ mm was used as wire electrode (Berkenhoff). Polished reference samples of all materials were manufactured conventionally by slicing bars of identical size using a diamond wheel. Sides were lapped and edges were carefully beveled. Eight eroded as well as eight polished bending bars were

produced. Fig. 1 shows schematically the manufacturing of the bending bars and the bending strength test.

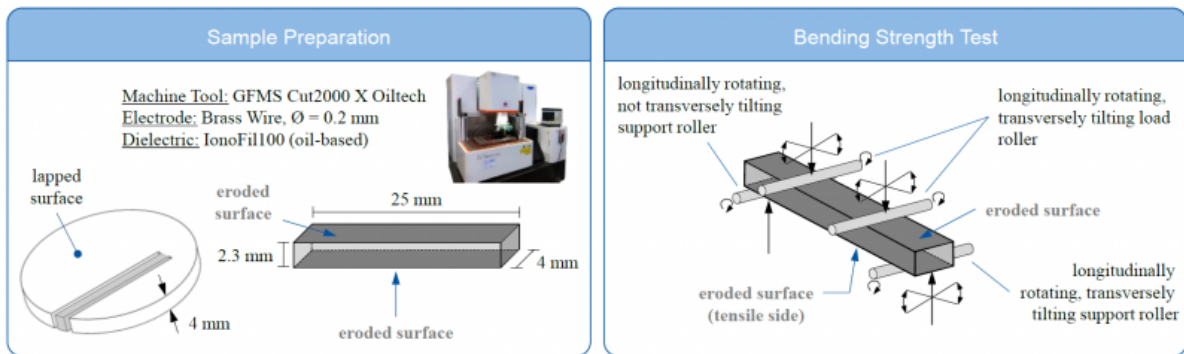


Fig. 1 Sample preparation and bending strength test

Due to the limited number of material specific machining technologies implemented on the machine (steel and cemented carbide), the steel technology applied had to be adapted in the main cut in order to enable a stable machining of the ceramics. The servo control value was used as an evaluation variable for stable machining, which adapts the feed control of the machine based on the resulting ignition delay time. In the machine control system, the servo reference value (S_{S011}) can be changed within limits of 0 – 70. The machine tries to reach this value during processing. With a data acquisition program from the machine tool manufacturer (which was made available exclusively for this purpose and is subject to confidentiality) it was possible to record the current servo value (S_{Ist}). If there are strong cyclical deviations between the set value and the current value during machining, this indicates unstable machining, which can result in low productivity or even wire breakage. The cutting rate served as a further evaluation parameter when adapting the machining technology. If there was a large fluctuation for S_{Ist} during machining of the ceramic, the S_{S011} had to be increased until the fluctuation decreased. At this point, the discharge frequency was increased via machine parameter P (adjustable between 0 – 70) to further increase the cutting rate. The higher the P value, the higher the discharge frequency. This parameter was increased until the fluctuation of the current servo value S_{Ist} increased. This resulting parameter set was used to manufacture the bending bars for the bending strength tests. This procedure was carried out for all ceramic compositions used for the tests, since the material systems had different electrical conductivities (see Table 2). Additionally a trim cut was used to improve the surface quality. For this investigation, the best results were achieved by using a trim cut with a very low discharge energy and a constant wire feed rate. The following table shows an overview of the machine parameters used at main cut (I, P, S_{S011}). Since the machine parameters do not represent real physical quantities, the averaged discharge current \bar{i}_e , the averaged discharge voltage \bar{u}_e and the discharge duration \bar{t}_e are listed as well, which are measured and determined by an oscilloscope (DPO7104C, Tektronix) and it's measuring equipment. The recorded discharge pulses were analyzed using a Matlab script. The arithmetic mean value of the respective parameter (\bar{i}_e , \bar{u}_e , \bar{t}_e , \bar{W}_e), with a maximum scatter of less than 2%, was determined from more than one million pulses (per ceramic). Furthermore, the electrical conductivities κ for all ceramics are listed, which were measured at room temperature.

Table 2: Material specific machine parameters used, resulting discharge parameters at main cut and electrical conductivity

Parameter	Material	0.5A 28WC	0.5A 32WC	0.5A 36WC	2.5A 28WC	2.5A 32WC	2.5A 36WC	5A 28WC	5A 32WC	5A 36WC	10A 28WC	10A 32WC	10A 36WC
I		5	5	5	5	5	5	5	5	5	5	5	5
P		35	50	50	35	50	55	40	45	50	40	45	50
S_{off}		65	65	65	50	55	60	50	55	60	50	55	60
\bar{i}_e / A		25.25	27.91	28.81	27.71	29.38	28.20	27.75	29.10	29.93	28.21	29.38	29.36
\bar{u}_e / V		68.13	69.83	69.19	64.36	67.03	70.04	64.18	62.81	63.49	64.11	65.03	69.21
$\bar{t}_e / \mu s$		1.162	1.131	1.125	1.195	1.097	1.124	1.155	1.112	1.096	1.126	1.138	1.087
$\kappa / (S/m)$		19.95	66.41	113.56	32.41	73.40	121.34	36.82	70.38	112.50	39.00	67.78	113.07

3 Experimental results

3.1 Conditions of wire electrical discharge machining process

The production of bending bars by wire EDM is mainly evaluated according to the productivity and stability of the machining process. The productivity is represented by the cutting rate and the stability of the machining is represented by the deviation of the current servo value S_{1st} . Fig. 2 (a) shows an overview of the cutting rate and the fluctuation of the servo value (arithmetical mean value) for the respective ceramic. Fig. 2 (b) shows the cutting rate with regard to the electrical conductivity, Fig. 2 (c) the cutting rate with regard to the fluctuation of the servo value and Fig. 2 (d) the discharge energy with regard to the electrical conductivity.

The results show that the cutting rates are very similar with only slight variations. If the cutting rate is considered in relation to the composition of the ceramics, only a slight dependence on the alumina content can be seen. The tungsten carbide content has no significant influence. With regard to the cutting rate and the electrical conductivity, no clear correlation can be seen, which was initially the hypothesis. This is in contrast to other investigations [1,10], where it was observed that the cutting rate is significantly dependent on the electrical conductivity of the material. The assumption is that either other material properties have a more significant influence on the machining conditions than the electrical conductivity, or that a conductivity orders of magnitude beyond the threshold ($\kappa > 1 - 10 \text{ S/m}$, [1]) may lead to a saturation effect. Observing the cutting rate plotted against the fluctuation of the servo value, a stronger influence can be seen. The cutting rate is reduced with increasing fluctuation. The 5A-36WC ceramic achieved a cutting rate twice as high as the 10A-36WC ceramic, although the same machine parameters were used. The adjustment of the machine parameters for stable machining of 10A-36WC ceramic was very complex. This suggests an unfavorable composition of this ceramic for machining via wire EDM. Since the thermal energy of electrical discharges is used for material removal, the analysis of the discharge energy is important to evaluate the process [11,12]. In relation to the rim zone evaluation, it can be estimated which energy level damages the rim zone too excessively. Furthermore, correlations with material properties can provide information about material removal. Based on the results in Fig. 2 (d), only slight correlations between the discharge energy and the electrical conductivity of these ceramics were observed. This consolidates the assumption that material properties such as thermal conductivity have a more significant influence on the process conditions.

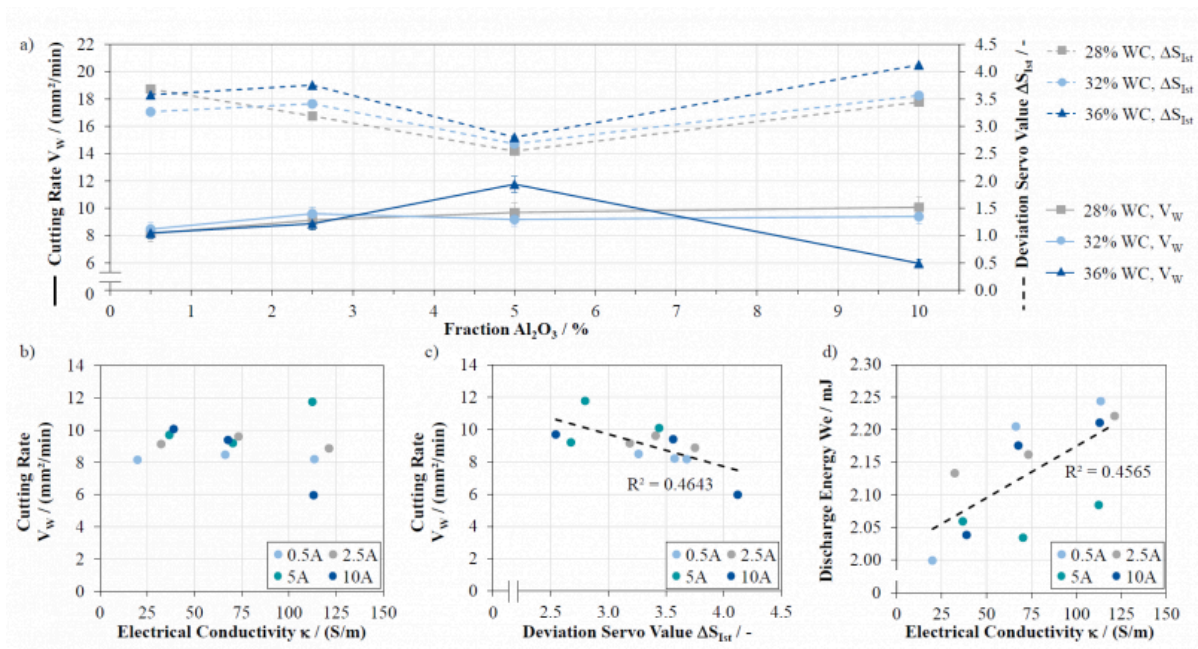


Fig. 2 Process conditions: (a) Overview of cutting rate and deviation of the servo value, (b) cutting rate with regard to electrical conductivity, (c) cutting rate with regard to deviation of the servo value, (d) discharge energy with regard to electrical conductivity

3.2 Bending Strength

In addition to the thermal and chemical durability of ceramics, mechanical strength is an important property. Every manufacturing process leaves a signature in the material surface [13–15], which has an influence on the mechanical properties of the material. Electrical discharge machining causes a thermally influenced rim zone, which depending on the removal mechanism of the material may have differing characteristics. Typical features are: micro-cracks, re-solidified material, pores or a microstructure transformation area.

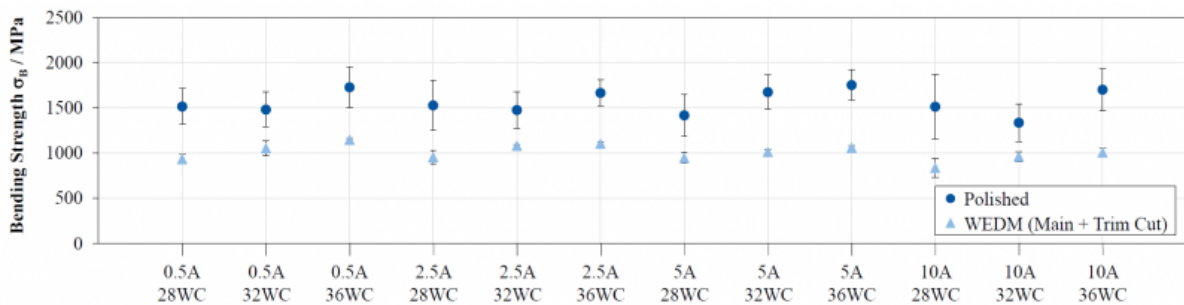


Fig. 3 Bending strength test results of WEDM and polished specimens

In the previous investigation [8], it was observed that the mechanical load capacity of a ceramic depends mainly on the discharge energies used and the resulting surface integrity. Here the influence of different material compositions on the mechanical load capacity using similar discharge characteristics is studied. Additionally, the results of eroded ceramics

are compared with those of polished reference samples (see Fig. 3). Furthermore, the previous study [8] demonstrates that the bending strength was significantly increased by using a trim cut with a very low discharge energy and a constant infeed of the wire. Hence, the bending bars were additionally machined with these trim cut parameters. Regardless of the manufacturing process, it can be seen that the bending strength is improved with increasing tungsten carbide content, but is reduced with increasing alumina content. This can be explained by the higher young's modulus of tungsten carbide ($E \approx 700$ GPa) in contrast to alumina ($E \approx 400$ GPa). It is necessary to determine the young's modulus/tensile strength of the respective ceramic in order to make a reliable conclusion. On average, the polished samples have a higher bending strength than the eroded samples, but the scattering of results is significantly higher. The assumption is that volume-related defects (material inhomogeneities) no process-related influences lead to the fluctuation of the bending strength of the polished specimens, because the surface is only slightly affected by the polishing process. In wire EDM, the induced residual stresses predominate, which is the reason for the lower bending strength. Nevertheless, more uniform rim zone conditions are present in comparison, which lead to less scattering.

4 Thermal simulation model

In recent years, efforts to predict the influence of a manufacturing process on material modification and the resulting component functionality have increased significantly. One approach is the modeling of process signatures using the finite element method (FEM) simulation of temperature fields during electrical discharge machining [14,16,17]. As the simulation of the continuous EDM process is very complex and not yet possible, it is necessary to define assumptions and simplifications to reduce the complexity. Therefore, a thermal simulation model based on a single discharge was used, which was built with COMSOL Multiphysics [18]. Input variables of the single discharge model are the characteristic process parameters discharge current, voltage and duration. Based on these parameters, the simulation model can calculate a heat source, which is applied to the surface of a 3D material model in a further step. The resulting heat transfer can be used to simulate the material removal per discharge and the temperature gradient in the microstructure below the discharge crater. A homogenized 2D material model was applied, since the ceramics used have three different phases, so the heat simulation would be considerably more complicated. It was applied for the 28WC and the 36WC ceramic. Alumina was neglected in the material model, because the focus was on the simulation of heat transfer in a ceramic containing only 0.5% alumina. The material parameters (phase transition temperature, melting enthalpy, etc.) had to be determined by Thermo-Calc based on thermodynamic database. Two energy levels were chosen for the simulation of the single discharges which correspond to the discharge energies from the previous study [8] ($We_1 = 1.3$ mJ & $We_2 = 4.27$ mJ), resulting in two time-dependent heat flux. Heat dissipation (e.g. into the dielectric) was taken into account. To estimate the modification of the material by EDM, the determined heat flux from the single discharge simulation were used for the heat transfer simulation in a 3D material model. For this purpose, a two-phase model was developed using a statistical volume element with an edge length of $10 \mu\text{m}$. The tungsten carbide grains were randomly distributed in the cube geometry representing the zirconia matrix using validated values.

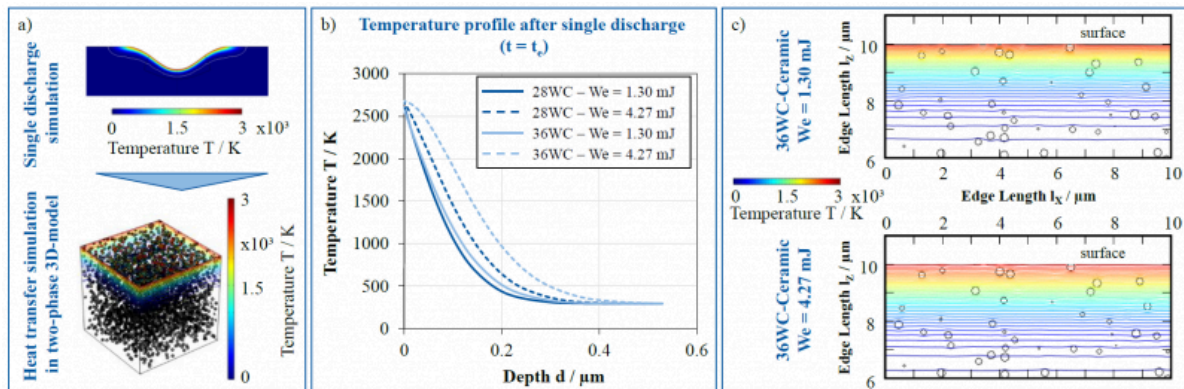


Fig. 4 Heat flow simulation: (a) Simulation model for single discharge and heat transfer in 3D-model, (b) temperature profile after single discharge in homogenized 2D-material model, (c) heat flux in two-phase 3D-model

The heat transfer simulation of the single discharges (Fig. 4) indicates that higher temperatures exist at certain depths in ceramics with a higher tungsten carbide content, regardless of the energy level. The heat flux transferred to the two-phase 3D-model (circles represent WC-grains) show that significantly wider temperature fields are present at the higher energies. For the 28WC-ceramic a similar characteristic with slightly lower temperatures at certain depths was found. In relation to the rim zone, which is analyzed in detail in the previous study [8], the higher temperatures and the wider temperature fields indicate a thicker rim zone at the higher discharge energy. In addition, a lower bending load capacity resulted at this energy level. Based on the heat transfer simulation, it may be assumed that the thickest rim zone is expected when machining the 36WC-ceramic with the high energy level and therefore a lower bending strength than with the low energy. Hence, machining the 36WC-ceramic with these discharge parameters is not appropriate with regard to the load capacity. This simulation model shows, that for different ceramic compositions and discharge parameters, the induced heat flow can be determined and thus a priori reliable process parameters can be predicted in a certain extent. In further investigations this must be verified by experiments and cross section analyses.

5 Conclusion and outlook

In this study, the electrical discharge machinability and the bending strength of electrically conductive alumina-zirconia-tungsten carbide (ATZ-WC) composite ceramics were investigated. No correlations could be identified between the cutting rate and electrical conductivity, which was initially the hypothesis based on the results of other researchers. However, a correlation between the cutting rate and the variation of the servo value could be determined. A minor fluctuation of the servo value indicates a high cutting rate (see Fig. 2 (c)).

Furthermore, the bending strength was determined for eroded as well as for polished samples. Depending on the material, the discharge parameters for main cut had to be adjusted. In addition, the samples were machined with a trim cut, which uses very low discharge energies and a constant wire feed. It could be observed, that independent of the manufacturing process the bending strength could be increased by increasing the tungsten carbide content and decreased by increasing alumina content. The reason could be the comparatively higher young's modulus of tungsten carbide. In addition to the experimental investigations, a heat transfer simulation model based on single discharge simulations was built. With this model it is possible to estimate to a certain extent the rim zone thickness caused by wire EDM. Since this simulation model cannot represent the entire wire EDM process, the simulation results are only indicative. Nevertheless, tendencies can be determined by comparison with experimental investigations.

In further research, additional materials to verified the model should extend the simulation model. Furthermore, other wire materials should be used in order to achieve an increase in cutting rate while retaining the same surface integrity.

Acknowledgements

The authors kindly acknowledge the funding by DFG Deutsche Forschungsgemeinschaft under the grant numbers BE 2542/21-3 and KE 879/3-3.

Bibliography

- [1] Panten U. Funkenerosive Bearbeitung von elektrisch leitfähigen Keramiken. Dissertation. Aachen. 1990.
- [2] Ferraris E, Vleugels J, Guo Y, Bourell D, Kruth J, Lauwers B. Shaping of engineering ceramics by electro, chemical and physical processes. *CIRP Annals* 65 (2). 2016. p. 761–784.
- [3] Pachaury Y, Tandon P. An overview of electric discharge machining of ceramics and ceramic based composites. *J. of Manuf. Processes* 25. 2017. p. 369–390.
- [4] Lauwers B, Kruth J, Liu W, Eraerts W, Schacht B, Bleys P. Investigation of material removal mechanisms in EDM of composite ceramic materials. *Journal of Materials Processing Technology* 149 (1-3). 2004. p. 347–352.
- [5] Saxena K, Agarwal S, Khare S. Surface Characterization, Material Removal Mechanism and Material Migration Study of Micro EDM Process on Conductive SiC. *Procedia CIRP* 42. 2016. p. 179–184.
- [6] Schmitt-Radloff U, Kern F, Gadow R. Wire EDM of ZTA-NbC Dispersion Ceramics – The Influence of ED Machining on Mechanical Properties. *Procedia CIRP* 68. 2018. p. 91–95.
- [7] Klocke F, Olivier M, Degenhardt U, Herrig T, Tombul U, Klink A. Investigation on Wire-EDM Finishing of Titanium Nitride Doped Silicon Nitride in CH-based Dielectrics. *Procedia CIRP* 77. 2018. p. 650–653.
- [8] Bergs T, Olivier M, Gommeringer A, Kern F, Klink A. Surface Integrity Analysis of Ceramics Machined by Wire EDM Using Different Trim Cut Technologies. *Procedia CIRP* 87. 2020. p. 251–256.
- [9] Gommeringer A, Kern F, Gadow R. Enhanced Mechanical Properties in ED-Machinable Zirconia-Tungsten Carbide Composites with Yttria-Neodymia Co-Stabilized Zirconia Matrix. *Ceramics* 1 (1). 2018. p. 26–37.
- [10] Gommeringer A, Schmitt-Radloff U, Ninz P, Kern F, Klocke F, Schneider S, Holsten M, Klink A. ED-machinable Ceramics with Oxide Matrix: Influence of Particle Size and Volume Fraction of the Electrical Conductive Phase on the Mechanical and Electrical Properties and the EDM Characteristics. *Procedia CIRP* 68. 2018. p. 22–27.
- [11] Klocke F, König W. *Fertigungsverfahren 3: Abtragen, Generieren Lasermaterialbearbeitung*. 4., neu bearbeitete ed. Springer-Verlag. Berlin, Heidelberg. 2007.
- [12] Yan M-T, Lai Y-P. Surface quality improvement of wire-EDM using a fine-finish power supply. *Intern. J. of Machine Tools and Manufacture* 47 (11). 2007. p. 1686–1694.
- [13] Brinksmeier E, Klocke F, Lucca D, Sölter J, Meyer D. Process Signatures – A New Approach to Solve the Inverse Surface Integrity Problem in Machining Processes. *Procedia CIRP* 13. 2014. p. 429–434.
- [14] Klocke F, Schneider S, Harst S, Welling D, Klink A. Energy-based Approaches for Multi-scale Modelling of Material Loadings During Electric Discharge Machining (EDM). *Procedia CIRP* 31. 2015. p. 191–196.

[15] Bergs T, Harst S. Development of a process signature for electrochemical machining. *CIRP Annals* 69 (1). 2020. p. 153–156.

[16] Weingärtner E, Kuster F, Wegener K. Modeling and simulation of electrical discharge machining. *Procedia CIRP* 2. 2012. p. 74–78.

[17] Hinduja S, Kunieda M. Modelling of ECM and EDM processes. *CIRP Annals* 62 (2). 2013. p. 775–797.

[18] Klocke F, Schneider S, Mohammadnejad M, Hensgen L, Klink A. Inverse Simulation of Heat Source in Electrical Discharge Machining (EDM). *Procedia CIRP* 58. 2017. p. 1–6.

PDF automatically generated on 2021-05-20 08:51:29

Article url: <https://popups.uliege.be/esaform21/index.php?id=4032>

published by ULiège Library in Open Access under the terms and conditions of the CC-BY License

(<https://creativecommons.org/licenses/by/4.0>)